



TENSILE FORCE ON FIXING BOLTS OF ELASTOMERIC ISOLATOR UNDER SHEAR DEFORMATION

Mineo TAKAYAMA¹, and Keiko MORITA²

SUMMARY

Laminated rubber bearings are fixed together a superstructure and a foundation by fixing bolts in many cases. The tension force of the bolts is generated only by the moment caused by shear force of the laminated rubber bearing. Though this fact has been predicted from the results of FEM, the verification by experiments has not been made. In this paper, the experiment was carried out in order to measure the magnitude of tensile force of the bolts, and the verification results of prediction equation of maximum tensile force were present. In addition, the factor influenced in the tensile force of the bolt was also examined by FEM analysis. By the experiment and FEM, it was clarified that the maximum tensile force of the bolt received the effect of the number of the bolts and rigidity of the flange plate, etc.. And, it was shown that the largest bolt tension can be estimated the according to the proposed equation by expecting to some extent margin.

INTRODUCTION

Laminated rubber bearing is widely used as an isolator for earthquake resistant structures in Japan. How can laminated rubber bearing demonstrate stable performance, holding compression loads under the condition of large horizontal deformation? This can be explained from the results of a finite element analysis (FEM analysis) of laminated rubber bearing. In short, as the pressure distribution within the laminated rubber bearing moves corresponding to the horizontal deformation, the laminated rubber bearing can demonstrate a stable horizontal deformation even under large deformation, by offsetting the $P-\Delta$ effect caused by supporting load (Takayama [1]).

It is presumed from the load-supporting mechanism of laminated rubber bearing that if the laminated rubber bearing is fixed to column by bolts, the tensile axial force extended to the bolts increase corresponding only to the bending moments caused by the shear force extended to the laminated rubber bearing, and it is not so great. From the FEM analysis including the flange and the bolts of laminated rubber bearing, the tension force extended to the bolts can be calculated from the bending moments mainly caused by shear force, and it is shown that the bolt axial force becomes the maximum when the compressive load is 0 (Takayama [2]).

¹ Associate Professor, Fukuoka University, JAPAN. Email: mineot@fukuoka-u.ac.jp

² Research Assistant, Fukuoka University, JAPAN. Email: keikomt@fukuoka-u.ac.jp

In this paper, bolt tensile forces were measured in actuality by experiment, the adaptability of the prediction equation for bolt tension force based on the FEM analysis was examined, and the contributing factors affecting to the generation of bolt axial force were considered.

OUTLINE OF SPECIMENS

Specimen of laminated rubber bearing

Two pieces of natural rubber bearing manufactured by Bridgestone Corporation were used as specimen, whose diameter was 500mm, rubber thickness was 3.4mm x 30 layers (total thickness of rubber 102mm), and insert plate thickness was 3.1mm. The first shape factor S_1 was 35.7, the second shape factor S_2 factor was 4.9, and the rubber material was the natural rubber equivalent to about 0.4MPa of shear modulus. The center hole size was 15mm, and the cover rubber (thickness 8mm) was integrated with the laminated rubber bearing in one unit. The diameter and thickness of the flange was 800mm and 20mm, respectively, and although the P.C.D (675mm) of the bolts were all the same, one specimen was an 8-hole type (E8 specimen) and another was a 12-hole type (A12 specimen). An A12 specimen is shown in Fig. 1.

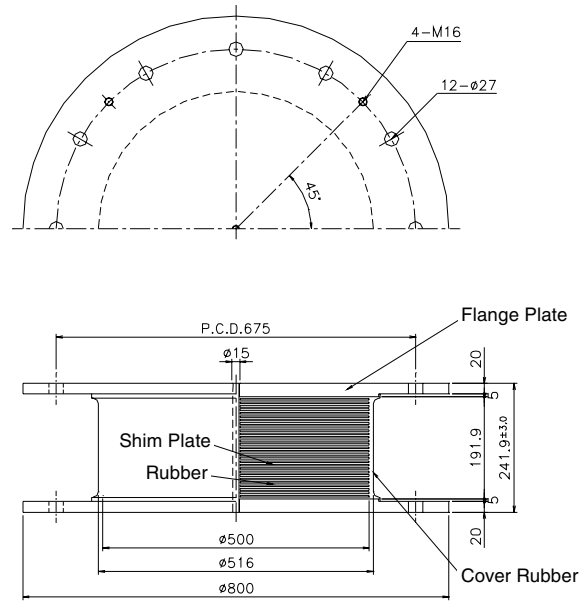


Fig.1 Rubber Bearing of A12 Specimen

Measurement of bolt axial force

To measure the axial force of the fixing bolt of the specimen, in order to minimize the effect on the bolt axial force, even if bending deformation occurred, the method to attach two strain gauges to sides of bolt was used. However, because the bolt tensile force generated was small, the shear force extended to the bolt exerted an adverse effect to the bolt axial force. Then, in order to detect just the bolt axial force without burdening the bolts with shear force, the special bolts that bear only the shear force of the specimen (hereafter called shear pins or set pins) were placed on two points of the excitation orthogonal axis (the axis (y) intersecting excitation axis (x) in a right angle).

The axial force generated on the fixing bolt was measured by the bolt (M24, SCM435) attached with strain gauges (product of Tokyo Measuring Instruments Laboratory Co. Ltd., FLA-5-11) on both its sides. The axial force extended to the bolt and the measurement value of the strain gauge were tested by the tensile test (maximum tensile load 100kN) beforehand, and their correction coefficients have been obtained. The set pins (SCM435, diameter 30mm) were fixed in the loading plate of the test equipment, and the void parts of the flange were filled with epoxy-based high-performance adhesion. It has been confirmed from the unit test conducted in advance that the strength of the adhesion used there was sufficient.

The bolts for the axial force measurement were only placed at the underside of the flange of the laminated rubber bearing. The alignment of the shear pins and the bolts for the axial force measurement are shown in Fig. 2. The bolt axial forces at six points on the lower flange of the 8-hole type and those at ten points

of the 12-hole type were measured. The remaining fixing bolts on the upper flange were fixed by bolts (M24) as usual.

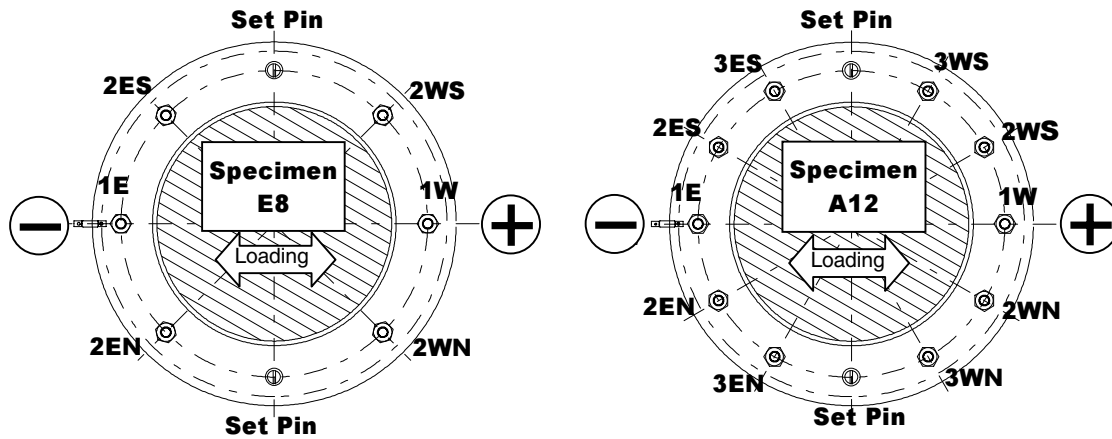


Fig.2 Layout of Bolts and Set Pins at Lower Flange

TEST METHOD

A large-scale, 2-axile test equipment (maximum compressive load of 32MN, horizontal load of 10MN, horizontal stroke $\pm 1000\text{mm}$) owned by Bridgestone Corporation was used. The structure of this equipment has the plate fixed with specimens sliding on the linear guide horizontally by an actuator. Compression tests and compression shear tests were conducted, both of which were static tests (excitation speed 13.3mm/sec. , triangular wave excitation).

The measurement of the initial value of data was made after the introduction of an initial torque of 40Nm [400kgf.cm] to the bolts, before fixing the upper zipper of the test equipment. The data were recorded at the interval of 5Hz .

Compression test

In the compression tests, loading from a tension stress of -0.5MPa (for A12 specimens) or -1MPa (for 8 specimens) to a compression stress of 20MPa were repeated in three cycles. In this compression test, the compression stiffness of the laminated rubber bearing was confirmed, and the axial force of the measuring bolt in the low tensile area was examined. In this paper, in principle, tensile load is expressed in minus numbers.

Compression shear test

From the condition of a given compression load, shear deformation was done repeatedly. The repeating number was 3 cycles. The maximum shear deformation was based on three steps as $\pm 102\text{mm}$ (shear strain 100%), $\pm 204\text{mm}$ (200%) and $\pm 306\text{mm}$ (300%). The compression stress was set in three steps as 1MPa , 10MPa and 20MPa . For the A12 specimen, in addition to the above excitation, the excitation of $\pm 408\text{mm}$ (400%) under a compression stress 1MPa was added.

RESULTS OF TEST

Compression test

Fig. 3 shows the relationship between the vertical loads and vertical displacements obtained from the compression tests. Although the relationship between load and deformation on the compression side showed high stiffness, those on the tensile side showed very low stiffness. The average compression stiffness between 1MN and 3MN on these hysteresis loops was calculated. The compression stiffness of A12 specimen was 1970MN/m and that of E8 specimen was 1990MN/m. As the specification of the laminated parts is the same, they showed almost the same compression stiffness.

If tensile stiffness is calculated as scant stiffness; the tensile stiffness of A12 specimens is about 120MN/m and that of E8 specimen is 80MN/m. As the E8 specimen has a large tensile deformation, it showed the influence of being softened. The tensile stiffness is about 1/16-1/24 of the compression stiffness.

Fig. 4 shows the comparison of total axial forces obtained from the vertical loads of the test equipment and the strain gauge measurement of the fixing bolts. Under the condition that the compression load is loaded, the generation of the bolt axial force is 0. Along with the increase of tensile load, the total bolt axial force increases almost proportionally (dotted line in the figure), although it shows a nonlinear movement. It can be said that up to approximately -0.1MN of the tensile load, the total bolt axial force is corresponding to the test equipment load. However, on the area with greater tension, the total bolt axial force greatly exceeds the test equipment load. Supposedly, it is because the bending deformation and other factors of the flange of laminated rubber bearing affected to the measurement of the bolt axial force.

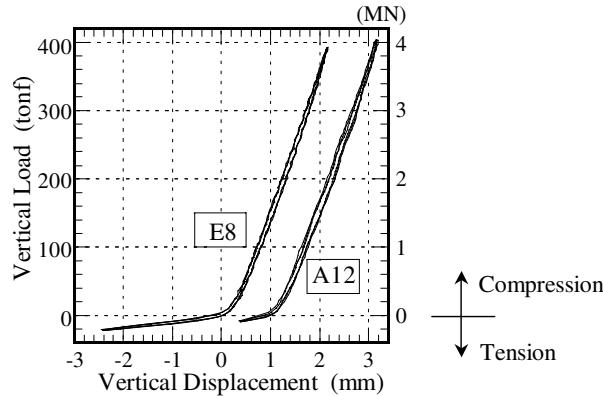


Fig.3 Compression Test Results

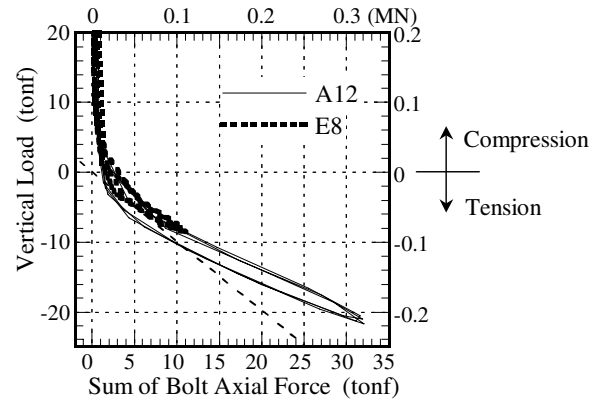


Fig.4 Bolt Axial Force obtained by Compression Tests

Compression shear test

Relationship between load and deformation

Fig. 5 shows the relationship between the horizontal load and horizontal displacement obtained from the compression shear test of A12 specimen, and also shows the relationship between the vertical displacement and the horizontal deformation. The reason the hysteresis area of the horizontal hysteresis loop looks large is that the horizontal load includes the friction force from the test equipment (linear guide). The horizontal hysteresis loops are drawn off the original point. With the increase in compression stress, the horizontal stiffness decrease slightly, and the hysteresis areas also become large. The hysteresis loop of E8 specimen is very similar to Fig.5.

With the increase in shear deformation, the vertical deformation increases (the compressive deformation is shown in minus in this figure only). Still, the vertical deformation is approximately 5mm when the shear strain is 300% under the stress 20MPa and is approximately 5% if it is converted to vertical strain.

From the horizontal hysteresis loop of Fig. 5, the horizontal stiffness was calculated. The horizontal stiffness was calculated as follows: obtain the shear forces under the shear strain $\pm 200\%$ ($\pm 204\text{mm}$) by both the loading curve and the unloading curve, and average the gradients of the straight lines between $+200\%$ and -200% . With larger compressive stress, the horizontal stiffness decreases slightly. The horizontal stiffness is approximately 0.8MN/m when the stress is 10MPa , and if it is converted to the shear modulus, it is $G=0.41\text{MPa}$.

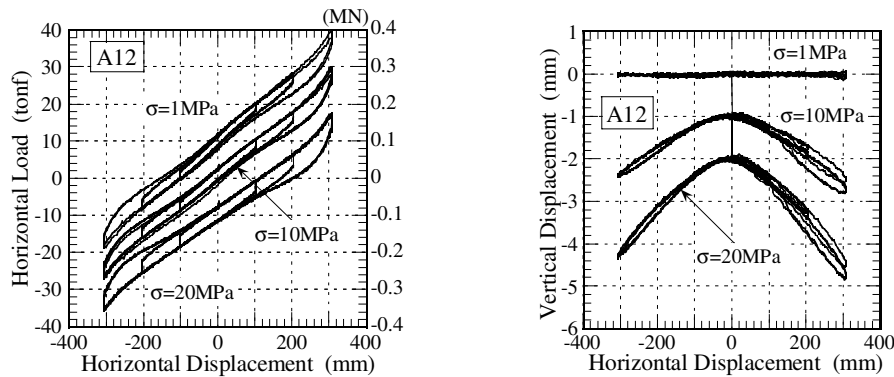


Fig.5 Hysteresis Loop obtained by Compression Shear Tests of A12 specimen

Bolt axial force

Fig. 6 shows the relationship between the bolt axial force and the horizontal displacement of the E8 specimen. Fig. 7 shows the test results of the A12 specimen. Figures show the right side and the left side of the bolts of each specimen separately. It is obvious that the axial forces are being generated in relating to the loading direction. With the increase in horizontal deformation, bolt axial forces also increase. (Refer to Fig.2)

The E8 specimen shows a slight difference in axial force by the difference of the bolt position. Up to approximately 100mm deformation, there has been no axial force greater than the initial axial force introduced. The more compressive stress increases, the more the bolt axial force decreases, and the lower the compressive stress is, the more the axial force is generated. The maximum axial force under the stress 1MPa is approximately 27kN when the horizontal displacement is in the plus side, about 23kN when it is in the minus side, and the average axial force is about 25kN .

Although the basic characteristics of the A12 specimen are the same as those of the E8 specimen, there is a difference in the axial force generated by each bolt. There is also a difference in the generation of axial forces between the plus side and the minus side of the horizontal displacement. The bolt generating the maximum axial force is 2WN in the minus side of the horizontal displacement and 2ES in the plus side, and the axial force is not generated symmetrically across the load centerline. Generally, it is assumed that the axial force in bolt positions (1E, 1W) farthest from the center of the specimen becomes the maximum. However, in A12 specimen, the bolts of both sides of them generate the maximum axial force. The maximum axial force is approximately 22kN as the average of the plus side and the minus side.

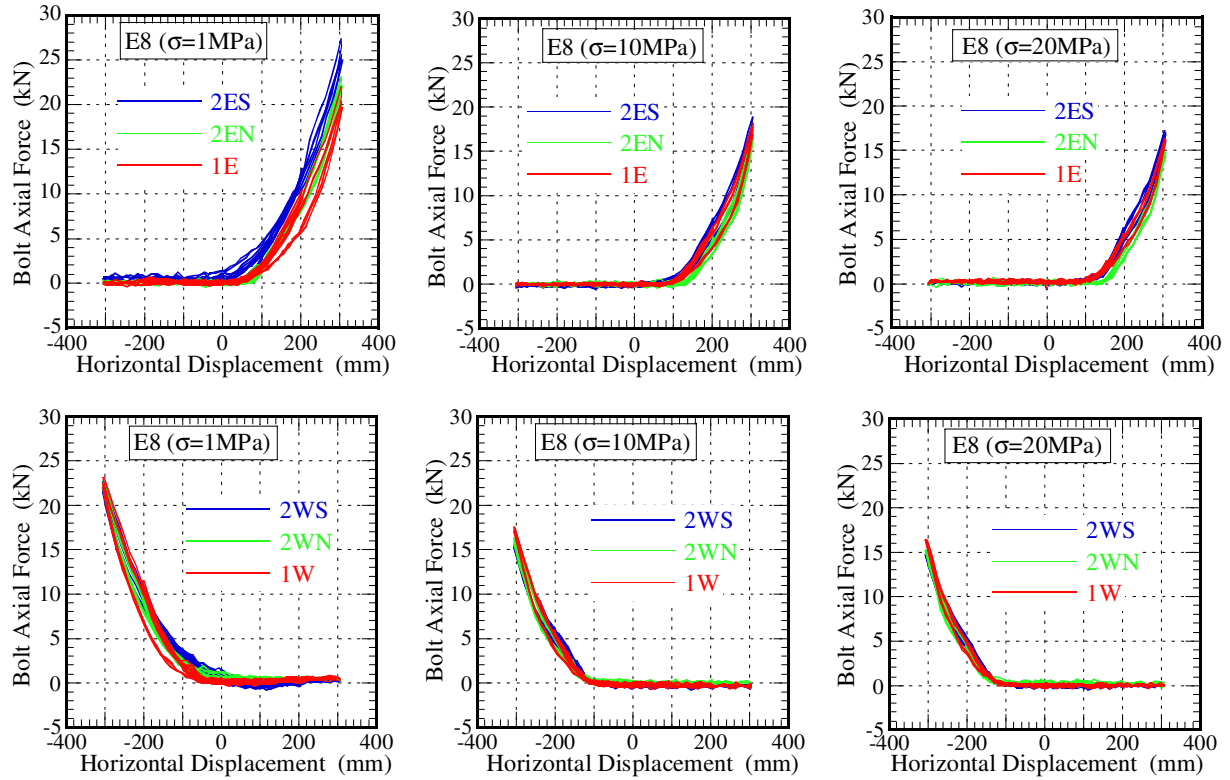


Fig.6 Relationship of Bolt Axial Force to Horizontal Displacement (E8 Specimen)

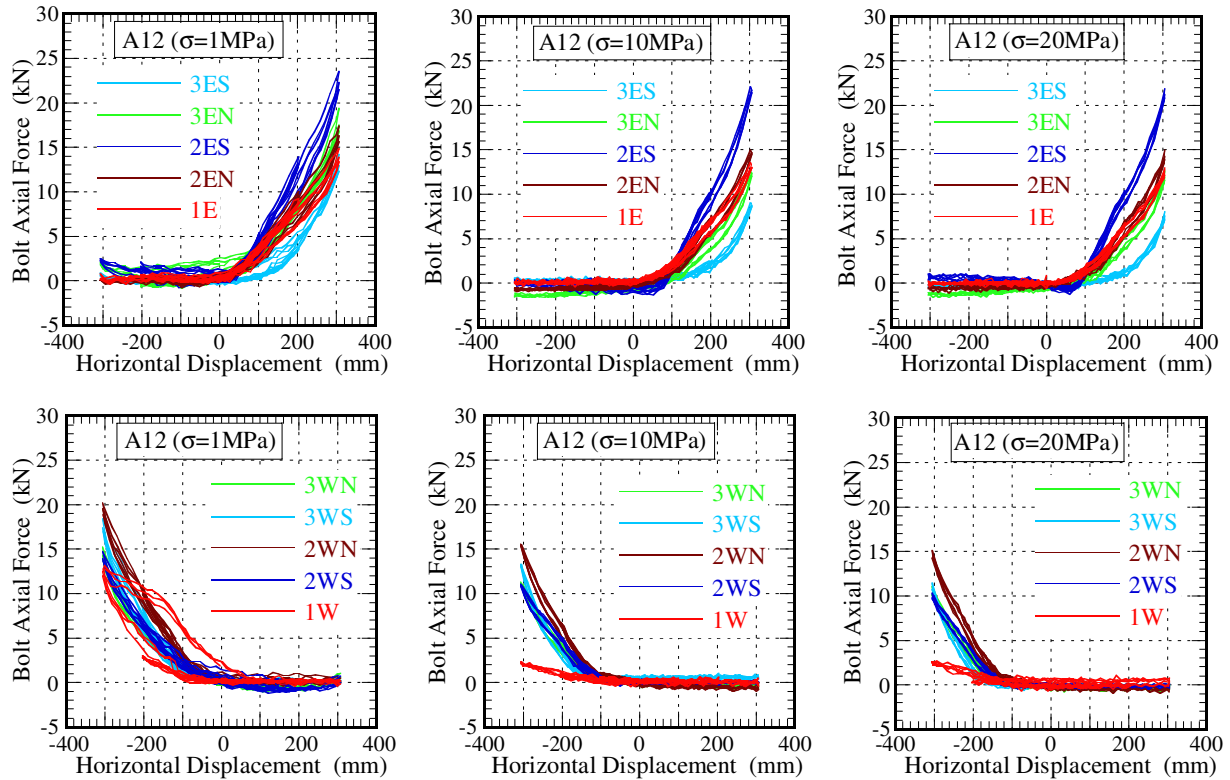


Fig.7 Relationship of Bolt Axial Force to Horizontal Displacement (A12 Specimen)

Despite that the number of bolts increased from 8 to 12, the maximum bolt axial force decreased approximately 12% only. It is assumed that the bolt axial force generated is influenced by the out-of-plane stiffness of the flange, the initial bolt axial force being introduced, etc., and the axial force borne by each bolt changes by the influence of them. The total bolt axial force calculated under a shear strain of 300% showed approximately 80-90kN as the maximum when the stress was 1MPa (the total bolt axial force is about 150kN when the shear strain is 400%). This is within the range in which the result of the measurement by a strain gauge in Fig. 4 does not become too nonlinear.

Prediction of bolt axial force

The prediction equation for the maximum bolt axial force based on a FEM analysis shown by Takayama [2] is as follows:

$$N_{pre1} = \frac{4Qh}{m(L + \delta)} \quad (1)$$

where, Q : shear force, h : total height of laminated rubber bearing (height of the specimen is 242mm), L : diameter between bolts (P.C.D) (675mm), m :number of bolts, δ :horizontal displacement

The equation (1) was derived from a balance between the moment by shear force and the moment by axial force of bolts. In equation (1), the center of the moment, which is obtained from bolt axial force, moves with the horizontal displacement δ . On the other hand, the equation for the bolt axial force of when the moment was calculated at the center of bolt alignment is as follows:

$$N_{pre2} = \frac{4Qh}{mL} \quad (2)$$

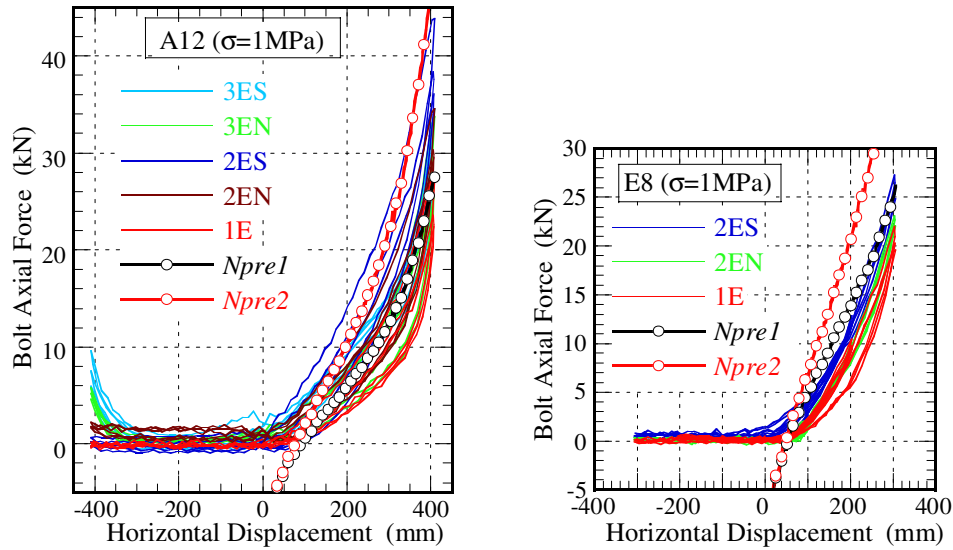


Fig.8 Comparison between Measured Bolt Axial Force and Prediction

Fig. 8 shows the relationship between the bolt axial forces measured and the predicted values of equation (1) and equation (2). At a deformation of 400mm of the A12 specimen, the bolt axial force increases greatly due to the influence caused by the hardening of the laminated rubber bearing. In the application of equations (1) and (2), for the shear force, Q , the data of the first cycle of the hysteresis loops obtained from the compressive shear tests were used. As the initial axial force (approximately 9kN) was introduced to the bolts in the test, the predicted values deducted by 9kN are compared with the experimental results

in Fig.8. In A12 specimen, the predicted values N_{pre2} correspond to the test results, and in E8 specimen, the predicted values N_{pre1} correspond more to the test results. Although equation (1) has been examined by a FEM analysis of the laminated rubber bearing with 8 bolts in Takayama [2], the case in which the number of bolts increased has not yet been examined. On this test, no significant differences in the axial forces were generated in bolts between the cases of eight bolts and twelve bolts. Presumably, it is because the mechanism of the bolt's burden of axial force was changed due to the increase in the number of bolts from eight to twelve.

From the results of this test, the axial forces generated in the bolts are within the ranges of equation (1) and equation (2), and it was confirmed that the maximum bolt axial force up to the shear strain around 400% can be largely predicted. However, as the bolt axial force generated is considered to be influenced by the number of bolts, the magnitude of the axial force initially introduced, the thickness of flange, etc., the quantitative assessments of these remain as future tasks.

FEM ANALYSIS

Analysis model

The analysis model was modeled based upon E8 specimen as close as possible. The analysis model was made as a 3-D model, and 1/2 of the specimen was modeled by 3-D eight node isoparametric elements, due to symmetric conditions.

Fig. 9 shows an analysis mesh. The rubber layer was divided into two in the direction of thickness, but the interlayer steel plate was not divided. The rubber bearing was divided at the distances of 30-35mm in the radius direction and into eight in the direction of circumference. The thickness of the flange is 25mm at the part of the laminated rubber bearing and 20mm at the peripheral part. Loading plates (steel) with 100mm thickness were connected to the upper and lower ends of the rubber bearing flange with GAP elements (an element that is stiff against compression, but does not resist tension).

Spring elements were aligned to the vertical direction between the loading plates and flanges only in the bolt's positions shown in Fig.9. The axial stiffness given to the spring elements was set as 300MN/m, using the M24 bolts' sectional areas and lengths (30mm) which were not constrained. Although actually, the bolts are introduced with an initial axial force, the initial axial force is 0 in this analysis. The spring elements are aligned in the positions in which set pins are aligned on the specimen.

By constraining the horizontal direction of the shear force between the nodal points where the spring elements are connected, the shear force from the loading plate can be borne by the flange. Frictions between the flange and the loading plate are ignored. The total number of nodal points of this model is 17822, and the total number of elements is 9920. The general purpose code MARC(K7.2) is used for the analysis.

Material modeling

Generally, rubber materials are modeled using the energy density function W . In this study, the equation (3) proposed by Ogden, which was improved to be able to take compressibility into consideration for rubber material modeling was used.

$$W = \sum_{n=1}^N \frac{\mu_n}{\alpha_n} \left[J^{\frac{-\alpha_n}{3}} \left(\lambda_1^{\alpha_n} + \lambda_2^{\alpha_n} + \lambda_3^{\alpha_n} \right) - 3 \right] + 4.5K \left(J^{\frac{1}{3}} - 1 \right)^2 \quad (3)$$

where, $J = \lambda_1 \lambda_2 \lambda_3$, λ_n is the principal stretch ratios, μ_n, α_n are material constants, and K is bulk modulus

[illegible]

N	1	2	3
μ_n	0.0101415	59.8582	25.9888
α_n	4.53727	0.00733436	0.0147159

$$G = \frac{1}{2} \sum_i \alpha_i \mu_i = 0.434 \text{ MPa} [4.34 \text{ kgf/cm}^2]$$

For the bulk modulus K , $K=2000\text{MPa}$ equivalent to approximately 5000 times of shear modulus G is used. Steel material was modeled for elasticity, and the model was given Young's modulus $E=210\text{GPa}$ and Poisson ratio 0.3.

Analysis method

After a given compressive load was loaded, a force-deformation (in the X direction, at 5.1mm step) was given to the nodal points at the uppermost surface in a monotonous way until the analysis became impossible. The compressive load was set as 0MPa, 1MPa, 10MPa and 20MPa as the compressive stress. All the nodal points at the lowermost surface of the loading plate are constrained to all directions. The central cross section (X-Z area) constrains the displacements on the orthogonal direction of the loads. The nodal points on the uppermost of the upper loading plate were constrained so that the displacements in the vertical direction became the same.

The case in which the number of bolts was doubled to 16 was analyzed, and the influence extended by the number of bolts was also examined. The analytic model of 8 bolts is expressed as S8 and that of 16 bolts is expressed as S16.

In order to assess the influence caused by the thickness of the flange, besides the flange thickness T_f of 20mm, the cases of flange thicknesses 10mm and 40mm were also analyzed. Although the setting value (300MN/m) of bolt axial stiffness was changed to 1/3, 3 and 10 times, maximum bolt axial force was changed only 4% approximately, so the effect of bolt stiffness to the generation of axial force is small.

Analytical results and discussion

Figure 10 shows the comparison of horizontal hysteresis and vertical displacement between the S8 model and the E8 specimen. The results of the analysis of horizontal hysteresis characteristics and vertical displacement are approximately the same as those of the experimental values. In the analysis on which the stiffness of the bolt and the thickness T_f of the flange were varied; there was no significant change in the hysteresis characteristics. From this fact, it can be said that the effect of the differences in the fixing parts to the hysteresis characteristics under the compressive-shearing condition of the laminated rubber bearing is small.

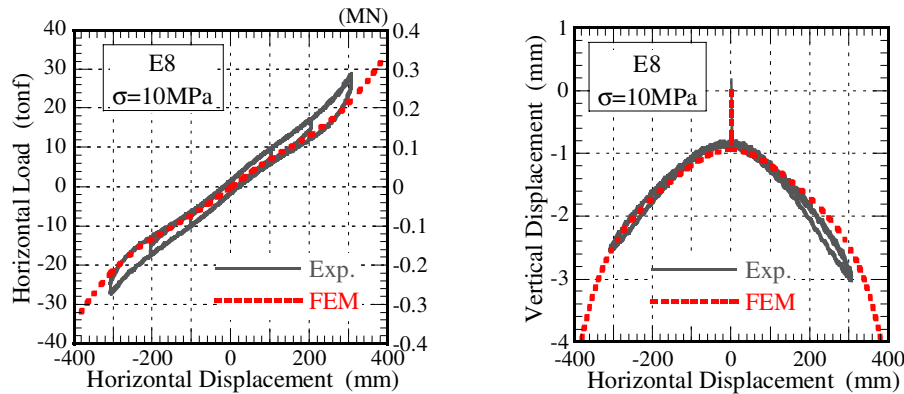


Fig.10 Hysteresis Loop obtained by FEM Analysis

Fig. 11 shows the axial forces of the bolts (spring) obtained from the FEM analysis. Refer to Fig. 9 for the Nos. of bolts. The thickness of the flange was 20mm. On the S8 model (left-hand side figures), the bolt axial forces on the excitation axial direction and its neighboring positions (No. 1 and 2) show approximately the same magnitude. The axial force of bolt No.3 on the excitation orthogonal axis increases with the increase in horizontal deformation. Although when the compressive stress is 0, the bolt axial force increases with the increase in horizontal deformation, when the compressive stress exists, the increase of axial force is kept low. Especially, under a stress over 10MPa, horizontal displacement is up to approximately 100mm and the generation of bolt axial force is very small. The more the stress increases, the more the generation of bolt axial force decreases. The maximum bolt axial force under the

horizontal deformation 300mm is +17% under the stress 0, -24% under 10MPa and -30% under 20MPa against the stress 1MPa.

The analytical results of model S16 (right-hand side figures) also has the same trend as the results of model S8, except that the bolt in which the maximum axial force is generated is not the bolt on the excitation axis (No.1), but its neighboring axis (No.2). This is the same trend as the test results of the A12 specimen, and when the number of bolts increases, the axial force borne by each bolt changes. The changes in the bolt axial force caused by the compressive stress are the same as the results of S8. The bolt axial force of S16 is approximately 1/1.5 of S8. Even if the number of bolts is doubled, the bolt axial force does not decrease proportionately.

In these figures, the predicted results of the bolt axial force from equations (1) and (2) are also shown. On the S8 model, N_{pre1} of equation (1) shows good correspondence, and on the contrary, on the S16 model, N_{pre2} of equation (2) also shows good correspondence. When the compressive stress increases on S16 model, the predicted value of equation (1) is nearer to the maximum bolt axial force. Supposedly, it is the sign of some changes incurred in the burden of the axial force borne by the bolt. In any case, from these tests and the results of the FEM analysis, the maximum bolt axial force is generated in the range of equations (1) and (2).

Although the bolt axial force by the FEM analysis and the measured bolt axial force by the test are not compared directly because of the influence of the axial force initially introduced, they are well corresponding to the prediction equations and the hysteresis characteristics of the laminated rubber bearing (Fig. 10), so, it can be said that the results of the FEM analysis are appropriate.

Figure 12 shows the relationship between the bolt axial force and horizontal displacement when the flange thickness was varied. The thicker the flange is, the more bolt axial forces decrease. If the bolt axial forces was compared under a horizontal displacement of 300mm, in the case of model S8, when the flange thickness is 10mm, the bolt axial force is +9%, and when the flange thickness was 40mm, the bolt axial force is -15% against that of when the flange thickness is 20mm. Likewise, in the case of the S16 model, when the flange thickness is 10mm, the bolt axial force is +16% , and when the flange thickness is 40mm, the bolt axial force is -23% against that of when the flange thickness is 20mm. It is revealed that in the case of the S16 model, the flange thickness was greater effect. In the case of the S16 model, when the flange thickness is 40mm, the generation of axial forces of bolt No.1 and bolt No.2 are approximately the same.

In the same figures, also, the prediction values of equations (1) and (2) are shown. In the case of S8 model, the thicker the flange is, the more the prediction value of the equation (1) moves to the safe side, and in the case of S16, the prediction value of the equation (1) comes closer to the analysis result than that of the equation (2). Supposedly, it was caused by the change of the bolt's burden of axial force because the flange had become stiff. The prediction equations are set to overpredict the tensile force.

At present, the thickness of the flange of the laminated rubber bearing product with about a 1000mm diameter is in the range of 30-40mm. If it is converted to the case of the specimen in this test by the ratio of the diameter, the thickness of its flange is equivalent to 15-20mm, and accordingly, the bolt axial force of the product is supposed to come closer to the result of the analysis of $T_f=10$ mm. In this case, as it is possible that the prediction value in a 300mm deformation range will be on the danger side, it is necessary to give some safety margin in the prediction equations.

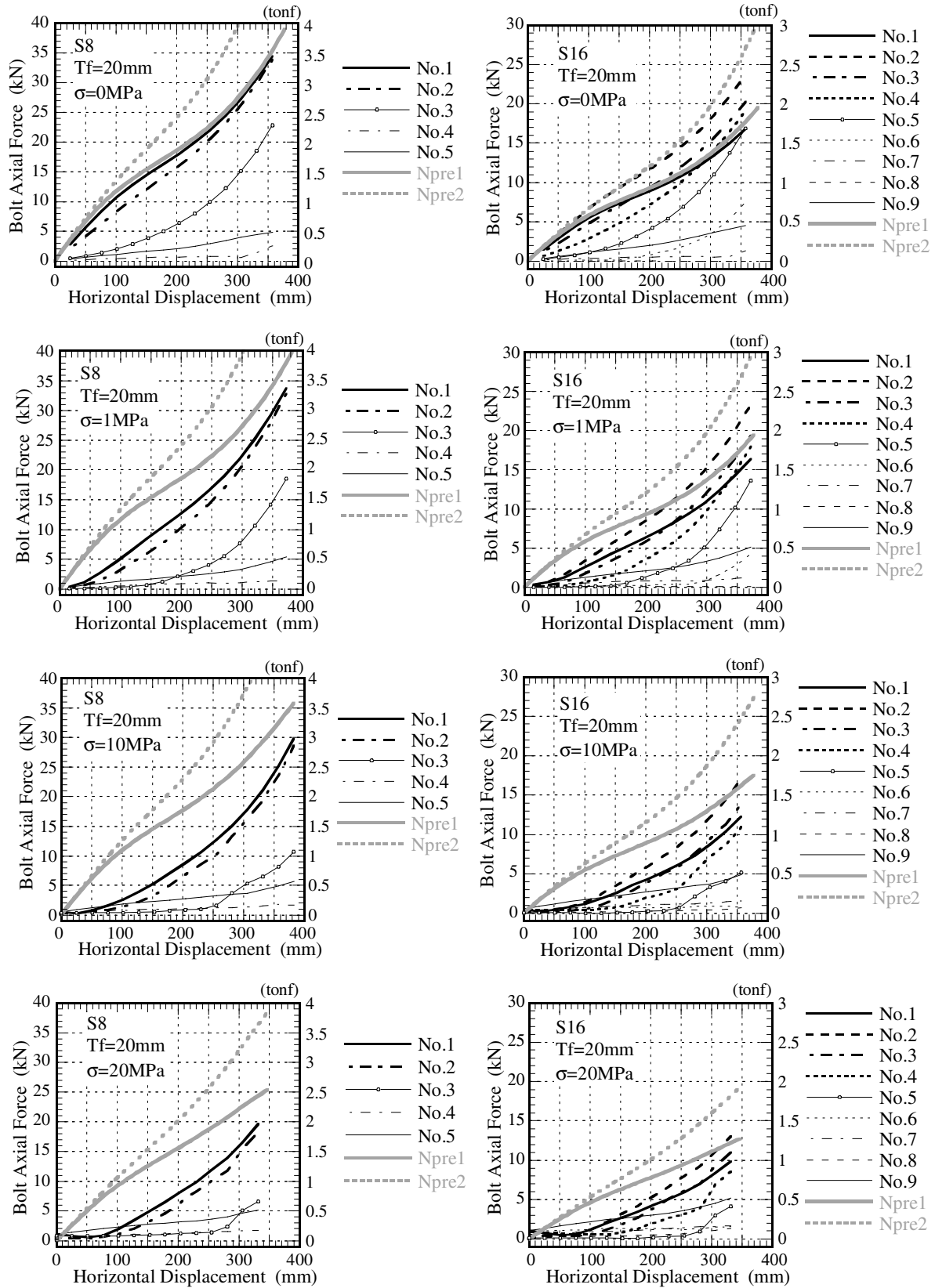


Fig.11 Bolt Axial Force obtained by FEM and Prediction Equation (Left:S8, Right:S16)

In the case that the number of bolts is smaller than that of this analysis range, although naturally the maximum axial force becomes great, the prediction is possible by properly applying the prediction equations. On the contrary, in the case that the number of bolts is larger than that of this analysis range, it is presumed that the maximum bolt axial force decreases. It is considered that the axial force can be predicted safely as the same as when the flange thickness is thin, by giving some safety margin in the prediction equations, taking into consideration that the proportion of the burden of tensile force will vary, influenced by the stiffness of the fixing parts.

In the laminated rubber bearing rupture event, it is assumed that greater axial force and shear force will be generated. It will be necessary to examine the safety of the bolt at the laminated rubber bearing rupture event separately. Regarding the adaptability of the prediction equations to the laminated rubber bearings other than that tested in this study (second shape factor S_2 is approximately 5), Takayama [2] shows that the prediction equations can be applied even in the case that the second shape factor S_2 is approximately 3.

Fig. 13 shows the deformation of the lower part of the flange, expanded to 200%, of when the shear strain is 300% in the case of the S8 model. The out-of-plane deformation of the flange decreases when the compressive stress works. It is revealed that when the thickness of the flange is around 40mm, the out-of-plane deformation rarely occurs. However, it is considered that the minor difference in deformation changes the proportion of the burden of bolt axial force. The maximum bearing stress of the flange at the time of this deformation was approximately 5 times of the average stress caused by the compressive load, which is the same as the result shown in Takayama [2].

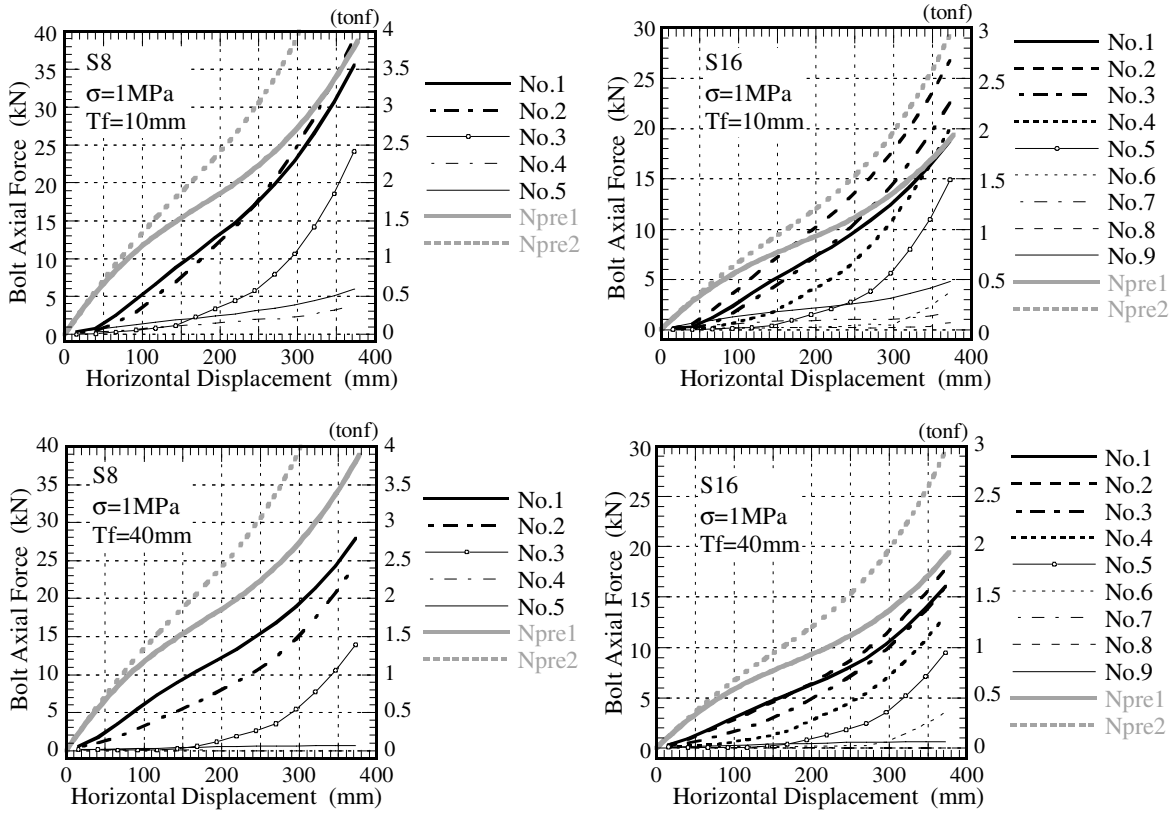


Fig.12 Bolt Axial Force obtained by FEM in Flange Thickness varied (Left:S8, Right:S16)

CONCLUSIONS

By the loading test focusing on the generation of axial force on the fixing bolts under the compressive shearing condition of the natural rubber bearing and by the simulation by the FEM analysis, the following knowledge was obtained:

- 1) The fact that the generation of axial force on the fixing bolt becomes the maximum when the compressive load is 0 from the previous analysis was verified by the experiment.
- 2) It was confirmed by the test and the FEM analysis that the effect extended to the horizontal hysteresis characteristics of the laminated rubber bearing from the difference of flange thickness is very small.
- 3) In the case that the number of fixing bolts was 12, the maximum bolt axial force was generated not on the bolt on the loading axis, but on its neighboring bolt. It was confirmed from the FEM analysis that when the flange was made thick, the bolt axial force decreased.
- 4) The maximum axial force of fixing the bolt can be predicted safely by equations (1) and (2). However, as it is considered that the axial force borne by the fixing bolt will vary according to the extents of the out-of-plane stiffness of the flange and the initial torque of the fixing bolt, it is important to give a safety margin to the predicted value to some extent.
- 5) In order to obtain the tensile force generated on the fixing bolts precisely, it is necessary to further examine about the laminated rubber bearing flange, its thickness, alignments of bolts, shapes of laminated rubber bearing and scale effects.

ACKNOWLEDGEMENT

We received good cooperation from Bridgestone Corporation and Okabe Struct Co., Ltd. in manufacturing laminated rubber bearing specimen and conducting the tests. We would like to express our thanks.

REFERENCES

1. Takayama, M., Tada, H. and Tanaka, R., "Finite-Element Analysis of Laminated Rubber Bearing used in Base-Isolation System", Rubber Chemistry and Technology, Vol.65, No.1, Rubber Division, ACS, 1992
2. Takayama, M., Morita, K., "Finite Element Analysis Focused on the Flange Plates and Connecting Bolts of Rubber Bearings", Proc. of 12WCEE, New Zealand, 2000

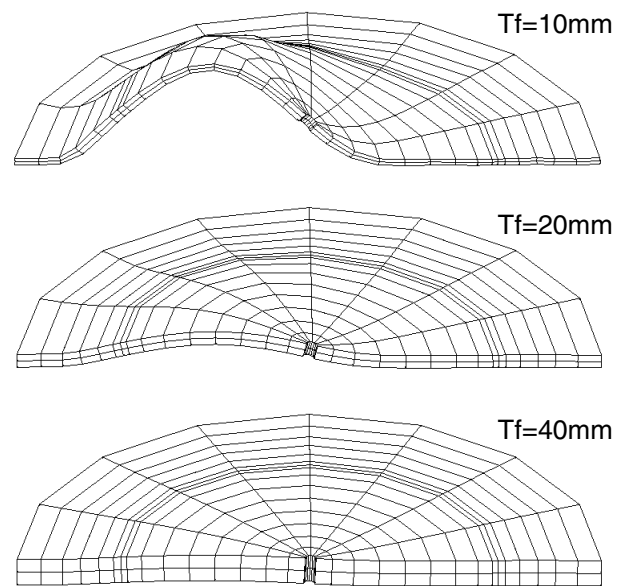


Fig.13 Deformation of Lower Flange
(S8 Model, Compressive Stress 1MPa)